Supplementary Information For

Rapid facile synthesis of Cu_2ZnSnS_4 nanocrystals

B. D. Chernomordik,[a] A. E. Béland,[a] N. D. Trejo, A. A. Gunawan, D. D. Deng,[a] K. A. Mkhoyan and E. S. Aydil*[a]

[a] Department of Chemical Engineering and Materials Science, University of Minnesota, Minneapolis, Minnesota 55455, United States.

Precursor Synthesis Procedures:

For **$Cu(dedc)_2$**: 150 mL of reagent alcohol was used to dissolve 9.0 g of sodium diethyldithiocarbamate trihydrate. Separately, 4.23 g of copper(II) chloride was dissolved in 50 mL of reagent alcohol. The carbamate-containing solution was then added dropwise to the copper chloride solution while stirring constantly. The resulting black precipitate was separated via filter, washed four times with ultra-high purity deionized water to remove unwanted salts, washed twice with cold acetone to remove the water, and finally dried in a desiccator under rough vacuum.

For **$Zn(dedc)_2$**: synthesis procedure is the same as that for $Cu(dedc)_2$, except that 3.38 g of zinc chloride (in lieu of copper(II) chloride) was used.

For **$Sn(dedc)_4$**: 140 mL of reagent alcohol was used to dissolve 9.6 g of sodium diethyldithiocarbamate trihydrate. Separately, 3.0 g of tin(IV) chloride was dissolved in 50 mL of regant alcohol. Following, as with the other two precursors, the carbamate-containing solution was added dropwise to the tin(IV) chloride solution while stirring constantly. The resulting orange precipitate was rinsed using copious amounts of deionized water followed by two rinses with ice-cold acetone. The orange precipitate powder was then dried in a desiccator with a roughing pump for at least one hour. At this point, purification by recrystallization of $Sn(dedc)_4$ is recommended because possible side reactions could form, for example, tin(II)-diethyldithiocarbamate. These impurities could affect the phase purity of the CZTS nanocrystals. To purify $Sn(dedc)_4$ by recrystallization, the orange precipitate, which was formed after dropwise mixing of the sodium diethyldithiocarbamate with tin(IV) chloride, was washed four times with ultra-high purity deionized water, twice with cold acetone, and subsequently dried in a desiccator. Following, the orange powder was dissolved in 800 mL of boiling acetone with vigorous stirring. The acetone solution was boiled until it turned cloudy (~650 mL remaining), at which point the flask was carefully removed from heat and allowed to cool to room temperature overnight. The flask was then cooled to -20 ˚C in a freezer and kept there for one day. The resulting precipitates and crystals were washed several times with ice-cold acetone and filtered to retain only the millimeter-sized reddish-orange crystals, which were dried in a desiccator under

rough vacuum and stored in a freezer. Yellow-orange crystals are undesired. Photograph(s) of the three precursor powders are shown in the Fig. S1.

Fig. S1. Photographs of the three precursors: (black) $Cu(dedc)_2$, (white) $Zn(dedc)_2$, and (red-orange) $Sn(dedc)_4$.

Discussion Regarding Addition of Oleic Acid for Dispersing Nanocrystals

The precipitation of nanocrystals via the addition of ethanol followed by centrifuging is referred to as "washing". If oleic acid (*e.g.*, 0.3 mL) is added to the dispersion before the second washing, the nanocrystals precipitate easily during centrifugation. In contrast, if oleic acid is not added prior to washing, a significant fraction of the nanocrystals remain dispersed despite aggregation as evidenced by a black and cloudy supernatant. Consequently, the yield of precipitated nanocrystals decreases drastically. We found that this observation may depend on the oleylamine supplier and the batch. For example, when one particular batch of oleylamine was used during the synthesis (Sigma Aldrich Lot No. BCBC6912), the nanocrystals could be precipitated with near 100% yield (clear supernatant) without the addition of oleic acid. The CZTS nanocrystals grown with different batches of oleylamines were indistinguishable from each other using the characterization techniques discussed in the manuscript, except in the atomic concentration of carbon in films cast from the nanocrystals as measured by EDS. Nanocrystal films have measurable amounts of carbon because of the presence oleic acid and oleylamine ligands on nanocrystal surfaces. The carbon concentration in films cast from nanocrystals synthesized using the BCBC6912 oleylamine was higher than the carbon concentration in films of nanocrystals synthesized using any other batch of oleylamine, when no oleic acid was used between washings and neat toluene was used to disperse the nanocrystals. For example, films of nanocrystals grown at 280 °C had ~20 at.% carbon when the BCBC6912 oleylamine was used, but films of nanocrystals grown using any other oleylamine had ~11 at.% carbon. In the latter films, the addition of oleic acid between the first and second washing procedures increased the carbon

concentration in the final films to ~14 at.%. The carbon concentration in films of nanocrystals was further increased to ~20 at.% by dispersing the nanocrystals in toluene that contained 0.01 vol.% oleic acid. While we have no definitive explanation for the differences between the oleylamine batches, it appears that impurities in the oleylamine may vary among batches and affect the surface chemistry of CZTS nanocrystals.

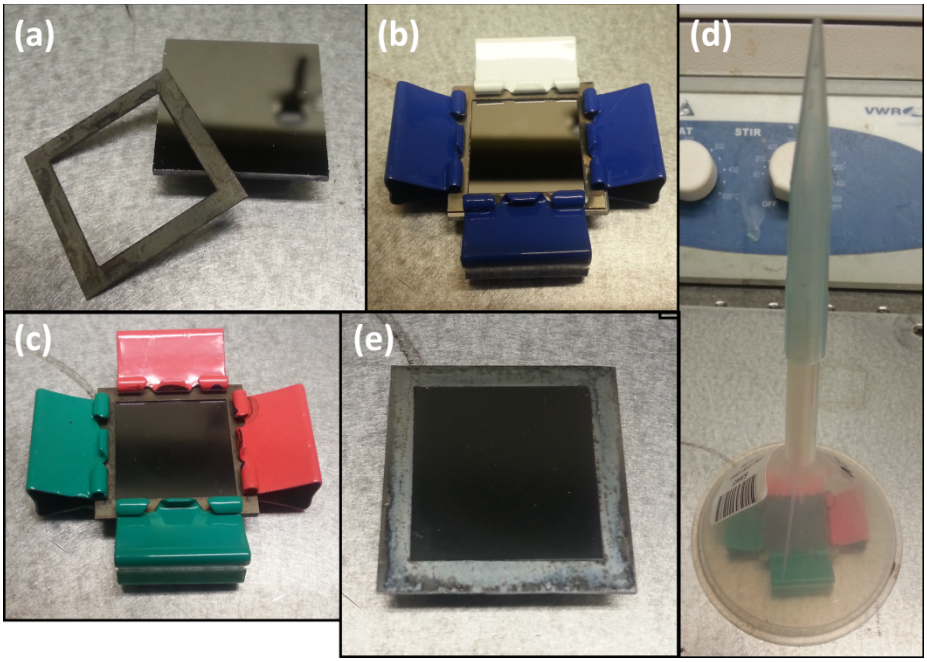

Fig. S2. Photographs depicting various stages of the film preparation procedure. (a, b) A frame is clasped onto a substrate, such as Mo-coated quartz; using binder clips. (c) The colloidal dispersion is then drop cast inside the frame. (d) A funnel is placed over the film during drying. (e) Finally, the binder clips and frame are removed to produce a nanocrystal film on the substrate.

Solar Cell Preparation and Characterization Details

For solar cells, the substrate was Mo-coated SLG. The Mo films were deposited using DC sputtering in two stages: ≈150 nm in 5 mTorr Ar with 250 W DC power applied to the target and then ≈250 nm in 1 mTorr Ar with 250 W DC power applied to the target. After annealing the CZTS films, a 185 nm CdS film was deposited on CZTS films with chemical bath deposition at 85 °C using an aqueous solution of 3 mM $CdSO_4$, 3 M NH_4OH, and 75 mM $(NH_2)_2CS$. The solution was stirred continuously at 500 rpm. The substrate was placed in the chemical bath at room temperature and the entire solution was heated to 85 ^oC. The deposition time was one hour. CdS deposition was followed by RF sputtering of 100 nm thick nominally intrinsic ZnO (i-ZnO) in 5 mTorr Ar and with 200 W RF power applied to the target. The deposition time was 27 minutes (*i.e.* the deposition

rate was ≈ 0.062 nm/s). Following, the substrate was heated to 150 °C for deposition of 250 nm of tin doped indium oxide (ITO) on the i-ZnO layer using DC sputtering in 5 mTorr Ar and with 150 W DC power applied to the target. The substrate was preheated to 150 °C for 10 minutes before ITO deposition. The deposition time was 27 minutes (*i.e.* the deposition rate was ≈0.15 nm/s). Finally, 50 nm of Ni and 1 μm of Al were sputtered sequentially in 5 mTorr Ar using 250 W and 200 W of DC power, respectively. The deposition times were 5 minutes and 156 minutes for Ni and Al, respectively; *i.e.* the deposition rates were ≈0.17 nm/s and 0.11 nm/s for Ni and Al, respectively. All films were sputtered in an AJA-ATC-2000 sputtering system. The base pressure of the sputtering chamber was $\approx 2.0 \cdot 10^{-6}$ Torr and the target to substrate distance was 19 cm. The substrate holder was rotated at 10 rpm. During ITO deposition, the substrate holder was heated with tungsten-halogen infrared lamps.

The current-voltage (J-V) characteristics of the solar cells were measured using a Keithley 2400 SourceMeter. The solar cells were illuminated using a 100 W Xe-arc lamp (Oriel) used in conjunction with a 0.125 m monochromator (Newport, Cornerstone 130). Two filters (Newport 81090 and 81092) were placed in between the lamp and the monochromator to simulate an AM1.5 spectrum. The monochromator was fitted with a 1200 groove/mm grating and a high reflectivity mirror. The mirror was selected to illuminate the solar cells with the broadband AM1.5 spectrum.

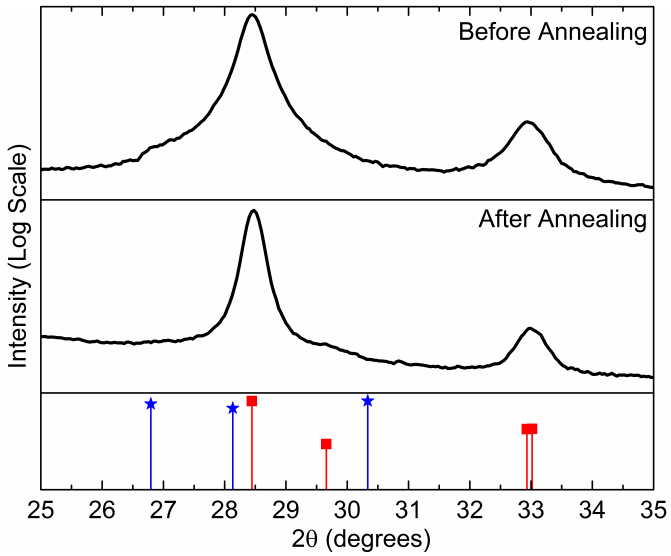

Fig. S3. XRD patterns for a film cast from ~24 nm CZTS nanocrystals, synthesized at 280 ˚C, (a) before annealing and (b) after annealing at 600 ˚C. The red, ■, symbols represent the diffraction pattern for kesterite CZTS (ICDD-ref 04-005-0388) and the blue, ★, symbols represent the derived wurtzite CZTS pattern.[1] The sample was annealed for one hour inside a sealed quartz ampoule with ~50 Torr of sulfur vapor present.[2]

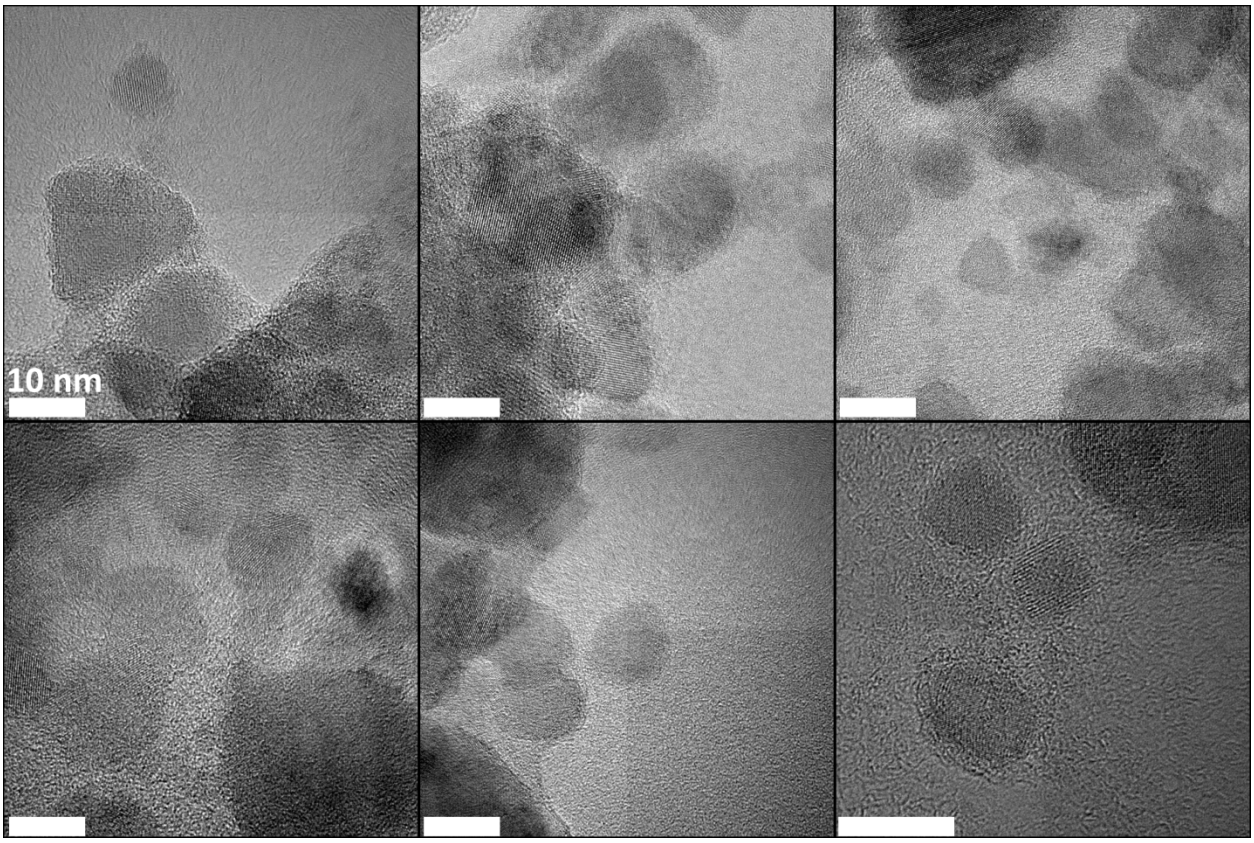

Fig. S4. Additional TEM images of nanocrystals synthesized at 280 ˚C. All scale bars are 10 nm.

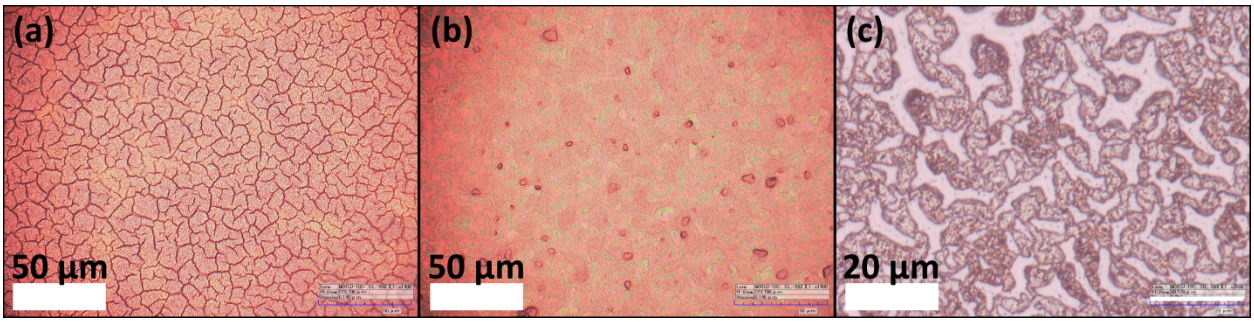

Fig. S5. Digital optical images of (a) a cracked film drop cast from a dispersion of ~5 nm CZTS nanocrystals in toluene, (b) a film cast using the same nanocrystals but with addition of a very small amount of oleic acid and (c) the same film after annealing at 600 ˚C in 50 Torr of S vapor. During annealing, the film shrinks due to nanocrystal coarsening and sintering and due to the decomposition and volatilization of the ligands. This shrinkage causes the formation of micron-scale cracks.

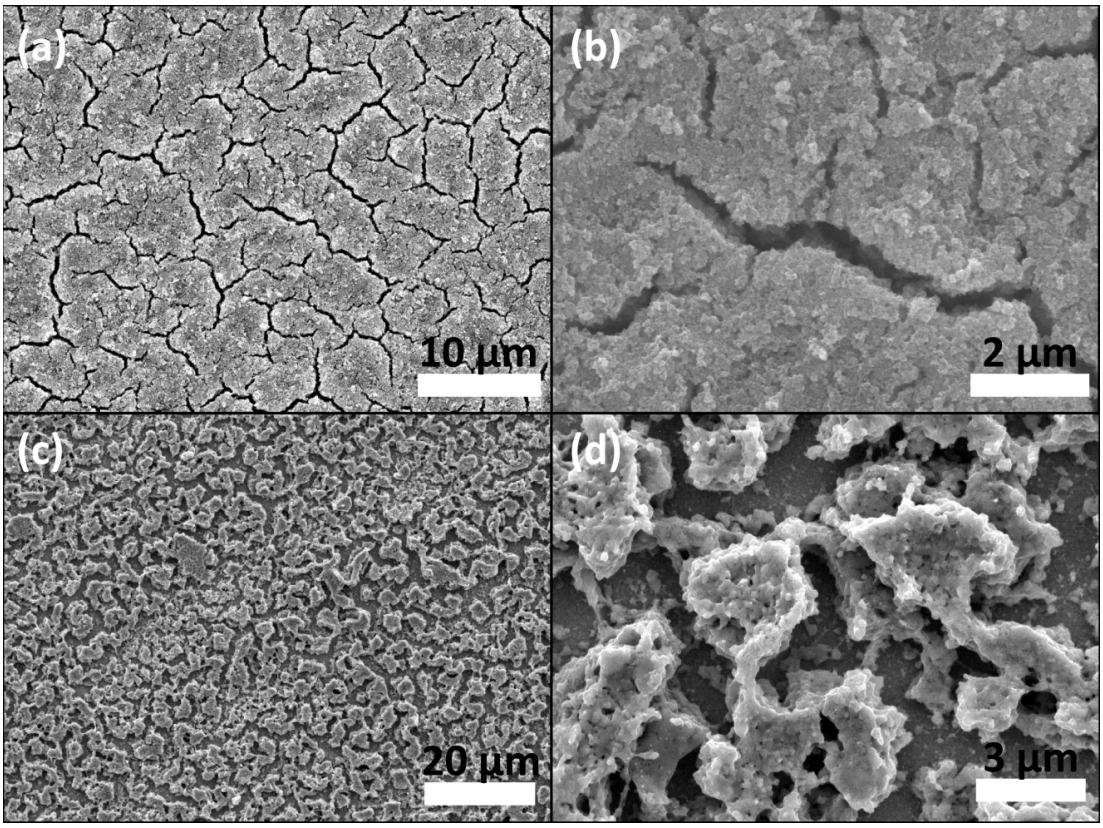

Fig. S6. (a, b) SEMs of a film deposited from a dispersion of 5 nm CZTS nanocrystals in toluene using a dip coating procedure similar to that used in reference [3]. The film exhibits nanometer-scale cracks. (c, d) These cracks grow during annealing at 600 ˚C in 50 Torr of S vapor.

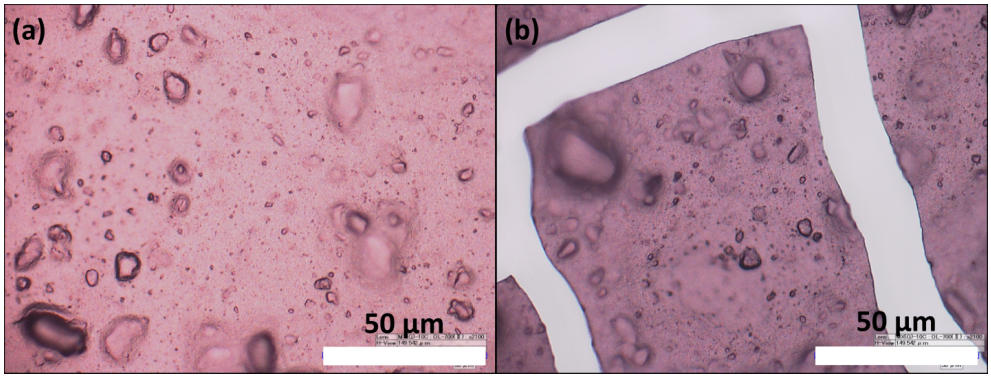

Fig. S7. (a) Digital optical image of a film comprised of 5 nm CZTS nanocrystals and deposited using doctor blading , where the solvent was hexanethiol and the solid loading was ~400 mg/mL (similar procedure reported by Guo *et al.*[4]). (b) The film cracks, due to volume loss, after heating on the hot plate at 300 ˚C for five minutes. The bumps in the film are nanocrystal aggregates.

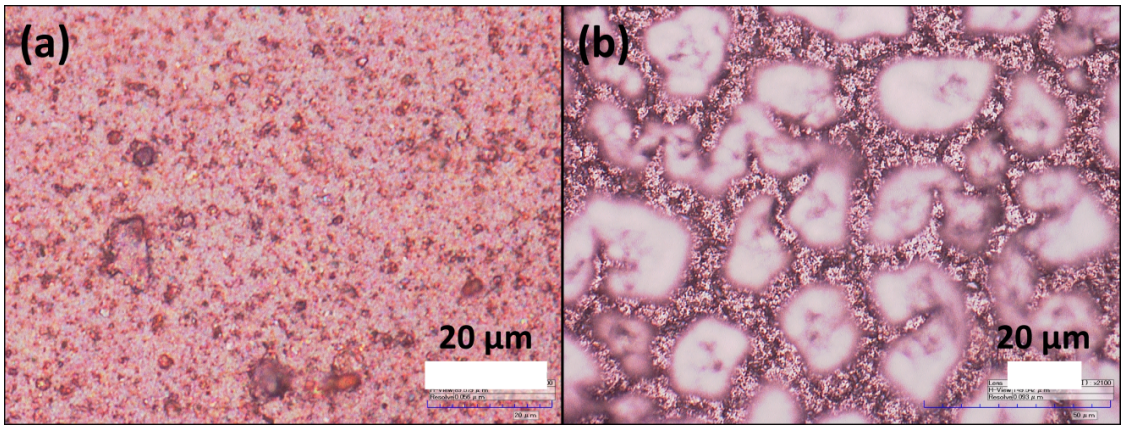

Fig S8. (a) Digital optical image of a film comprised of ~13 nm CZTS nanocrystals deposited using doctor blading as in Fig. S7 but the deposition was done in two steps: two layers were deposited with drying on a hot plate at 300 ˚C for five minutes in between each layer. (b) The film in (a) after annealing at 600 ˚C in 50 Torr of S vapor. The film cracks, forming large islands at the top of the film.

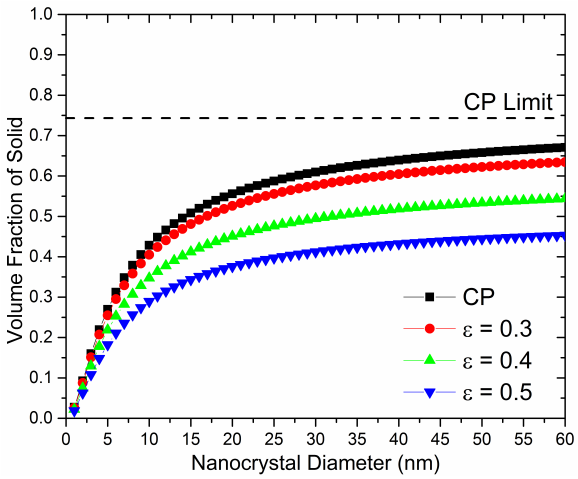

Fig. S9. The dependence of the solid volume fraction on the nanocrystal diameter in a film comprised of nanocrystals covered with a 1 nm thick ligand shell for several different porosities (ε) down to the close packed (CP) limit (ε=0.26).

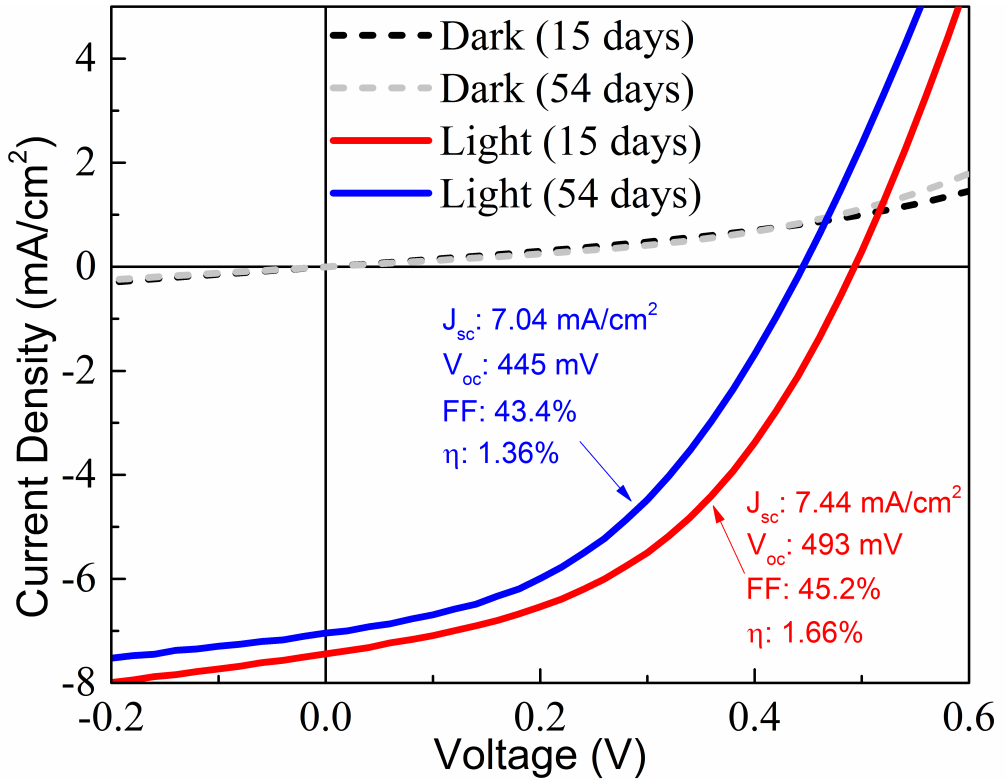

Fig. S10. J-V curves for the solar cell device shown in Figure 6f for two different time periods after fabrication. The J-V characteristics in Figure 6f were collected 15 days after fabricating the device and the characteristics are reproduced here as the red curve. The same device was measured again a total of 54 days after fabrication and the J-V characteristics are shown in blue.

References

1. X. Lu, Z. Zhuang, Q. Peng, and Y. Li, *Chem. Commun.*, 2011, **47**, 3141–3143.
2. B. D. Chernomordik, A. E. Béland, D. D. Deng, A. A. Gunawan, D. J. Norris, and E. S. Aydil, *Chem. Mater.*, submitted (2014).
3. J. M. Luther, M. Law, Q. Song, C. L. Perkins, M. C. Beard, and A. J. Nozik, *ACS Nano*, 2008, **2**, 271–280.
4. Q. Guo, G. M. Ford, W.-C. Yang, B. C. Walker, E. A. Stach, H. W. Hillhouse, and R. Agrawal, *J. Am. Chem. Soc.*, 2010, **132**, 17384–17386.